Smecticlike rheology and pseudolayer compression elastic constant of a twist-bend nematic liquid crystal

M. Praveen Kumar [1], P. Kula,[2] and Surajit Dhara [1,*]

[1]*School of Physics, University of Hyderabad, Hyderabad 500046, India*
[2]*Institute of Chemistry, Faculty of Advanced Technologies and Chemistry, Military University of Technology, Warsaw, Poland*

In twist-bend nematic (N_{TB}) liquid crystals (LCs), the director (mean molecular orientation) exhibits heliconical structure with nanoscale periodicity. On the mesoscopic scale, N_{TB} resembles layered systems (like smectics) without a true mass density wave, where the helical pitch is equivalent to a "pseudolayer." We study rheological properties of a N_{TB} phase and compare the results with those of a usual smectic-A phase. Analyzing the shear response and adapting a simplified physical model for the rheology of defect-mediated lamellar systems, we measure the pseudolayer compression elastic constant B_{eff} of the N_{TB} phase from the measurements of the dynamic modulus $G^*(\omega)$. It is found that B_{eff} of the N_{TB} phase is in the range of 10^3–10^6 Pa and it follows a temperature dependence, $B_{eff} \sim (T_{TB} - T)^2$, as predicted by the recent coarse-grained elastic theory. Our results show that the structural rheology of N_{TB} LCs is strikingly similar to that of the usual smectic LCs, although the temperature dependence of B_{eff} is much faster than that of smectic LCs as predicted by the coarse-grained models.

I. INTRODUCTION

Experimental discovery of the twist-bend nematic (N_{TB}) phase in bent-core liquid crystals has created immense interest in the liquid crystal community [1–7], although it was theoretically predicted much earlier from different perspectives [8–11].

In the N_{TB} phase, the director $\hat{\mathbf{n}}$ (the mean molecular orientation) exhibits periodic twist and bend deformations forming a conical helix and is tilted with respect to the axis $\mathbf{L}$, as shown in Fig. 1(a). The typical pitch p of the heliconical structure is of the order of 10 nm, thus comparable to a few molecular length. Commonly, the N_{TB} phase is observed in odd-membered liquid crystal dimers wherein two mesogenic units are connected through a flexible spacer [12–14].

A fascinating feature of the N_{TB} phase is the observation of spontaneous chirality i.e., formation of both left- and right-handed helical domains even though the constituent molecules are achiral. This leads to several unusual physical properties of the N_{TB} phase compared to the conventional nematic phase (N) [15–21].

A few coarse-grained theories have been proposed to explain the emergence of the N_{TB} phase from the high-temperature uniform nematic phase. Meyer and Dosov showed that the elastic properties of the N_{TB} phase could be viewed in two different length scales in reference to the pitch length p [22]. When the considered length l is less than p, i.e., $l < p$, the elastic description is similar to that of the usual nematics. On the other hand, when $l \gg p$, the elastic description is similar to regular lamellar systems such as cholesteric and smectic liquid crystals (LCs) [22]. In the latter picture, the thickness of one pitch can be considered a pseudolayer, and the large-scale elasticity of the N_{TB} phase can be described in terms of an effective pseudolayer compression elastic constant B_{eff} and an curvature elastic constant K_{11}^N, and the corresponding free-energy density of N_{TB} can be expressed as [22]

$$f_{TB} = \frac{1}{2}B_{eff}\epsilon^2 + \frac{1}{2}K_{11}^N\left(\frac{1}{R_1} + \frac{1}{R_2}\right)^2, \qquad (1)$$

where ϵ is the pseudolayer compression and R_1 and R_2 are the curvatures. Another coarse-grained theory was developed considering the helipolar order and it's coupling with bend distortions [20,23]. Both theories predicted that the temperature dependence of B_{eff} is much faster than that of the usual smectic-A (Sm-A) LCs.

There have been very few experimental studies on the measurements of B_{eff} of N_{TB} LCs [23–25]. For example, Gorecka *et al.* measured B_{eff} of CB7CB and some chiral N_{TB} LCs. Their reported values are in the range of a usual Sm-A LC (10^6–10^7 Pa) and vary inversely with the temperature [24]. Parsouzi *et al.* reported that B_{eff} is in the range of 10^3–10^4Pa and it scales as $B_{eff} \sim (T_{TB} - N)^{3/2}$ [23]. Thus, a several orders of magnitude difference in the reported values, measured on two different samples using two different methods and its universal temperature dependence, is still an unresolved problem. In this paper we report experimental studies on the rheological properties of a N_{TB} LC. We use a method for measuring B_{eff} from the dynamic shear modulus $G^*(\omega)$. We discuss the temperature dependence of B_{eff} and compare it with that proposed by the coarse-grained elastic theories of the N_{TB} phase.

II. EXPERIMENTAL

The LC material 1,ω-bis(4-cyanobiphenyl-4′-yl) alkane (CB9CB) was synthesized in our laboratory. It is a
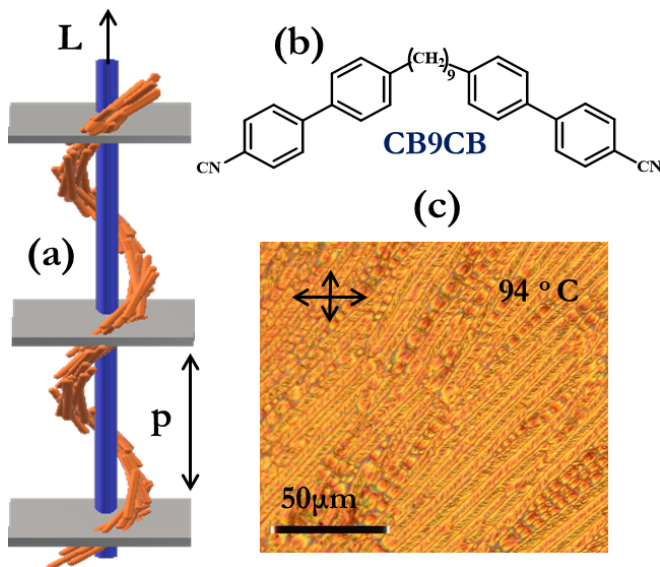
*sdsp@uohyd.ernet.in

FIG. 1. (a) Schematic view of the heliconical molecular orientation of the nematic twist-bend (N_{TB}) phase. p represent helical pitch equivalent to pseudolayer thickness. (b) Chemical structure of CB9CB molecules used in the study. (c) Polarizing optical microscope texture at 94 °C in the N_{TB} phase. **L** is the macroscopic average orientation of $\hat{n}$ over several periods.

cyanobiphenyl-based dimer with an odd number of methylene units ($n = 9$) in the flexible spacer [Fig. 1(b)]. It exhibits the following phase transitions: isotropic I 124 °C to N 108 °C to N_{TB} 84 °C to crystalline (Cry) and an enantiotropic transition with the widest temperature range of the N_{TB} phase 22 °C among the LCs in the homologous series of CBnCB [14]. For the purposes of comparison we also studied 8CB (octylcyano biphenyl), which shows the following phase transitions: I 41 °C to N 34 °C to Sm-A 22 °C to Cry. We used a strain-controlled rheometer (MCR 501, Anton Paar) with a cone-plate measuring system with a plate diameter of 25 mm and cone angle of 1° for rheological measurements. A Peltier temperature controller was attached to the bottom plate to control the temperature with an accuracy of 0.1 °C. A hood was used to cover the measuring plates for uniformity of the sample temperature. Temperature-dependent viscosity was measured in cooling the sample from the isotropic phase. To measure the dynamic shear modulus the sample was quenched from the isotropic to the N_{TB} phase at a rate of 15 °C/min. A total of 5 g of LC was synthesized, and about 200 mg were used for each rheological measurements. Initially, the phase transitions and textures were observed using a polarizing optical microscope (Olympus BX51) and a temperature controller (Mettler FP 90). A typical texture of an unaligned sample is shown in Fig. 1(c). It is noticed that the texture of N_{TB} is very similar to that of the focal conic textures of the usual Sm-A LCs.

III. RESULTS AND DISCUSSION

To begin with we measure the shear viscosity of CB9CB as a function of temperature at two shear rates ($\dot{\gamma} = 100$ and 10 s^{-1}) to identify the phase transition temperatures. Since the
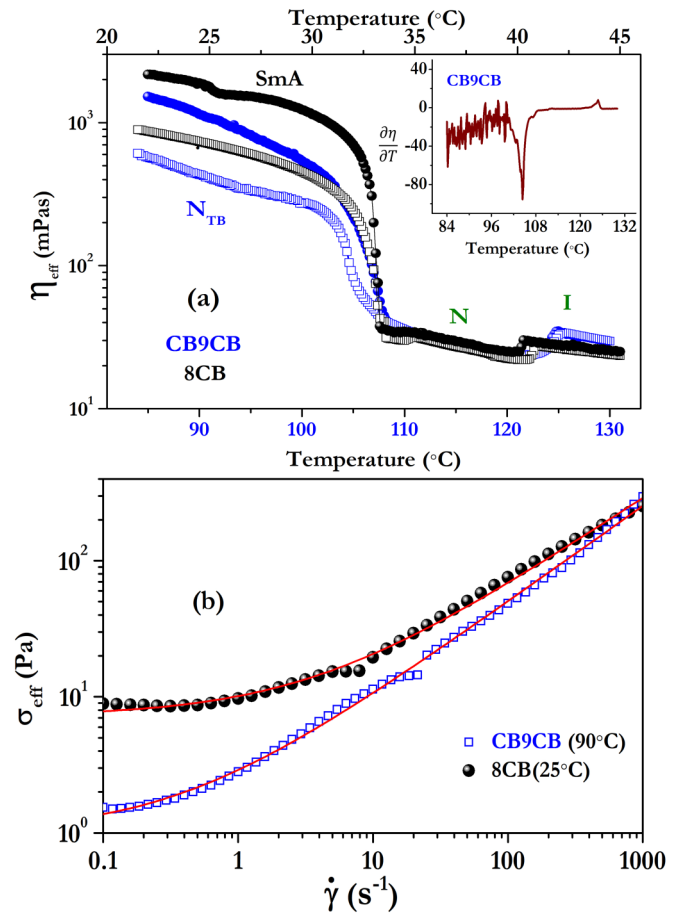

FIG. 2. (a) Temperature-dependent effective viscosity η_{eff} of CB9CB (blue squares) and 8CB (black spheres) LCs at two different shear rates, namely, $\dot{\gamma} = 100$ s^{-1} (squares) and $\dot{\gamma} = 10$ s^{-1} (circles). Inset: Variation of $\frac{\partial \eta_{eff}}{\partial T}$ with temperature T of CB9CB. (b) Shear-rate-dependent effective shear stress σ_{eff} at fixed temperatures. The solid lines are theoretical fits to Eq. (2).

orientation of the director with respect to the shear direction usually changes with temperature, we define it as effective viscosity η_{eff}. As shown in Fig. 2(a), the N to N_{TB} transition is identified from the rapid increase (more than two orders of magnitude) of η_{eff} with respect to the N phase. The onset of the N-N_{TB} transition (108 °C) is better seen in the inset of Fig. 2(a). We also measured the temperature-dependent η_{eff} of 8CB LC, as shown in Fig. 2(a). It is evident that the magnitude and the overall temperature dependence of η_{eff} of the two samples are very similar. This similarity also presumably indicates that the pretransitional fluctuations and the resulting director dynamics across the N-N_{TB} transition are similar to that of the N-Sm-A transition [26–28]. In analogy with 8CB LC, the three simplest orientations of the pseudolayers can be considered, wherein the layer normals are parallel to the vorticity $\nabla \times v$, velocity gradient ∇v and flow directions v, as shown schematically in Fig. 3. These are commonly known as perpendicular, parallel, and transverse orientations. The large η_{eff} of the N_{TB} phase is expected to arise from the transverse orientation of the pseudolayers, similar to those reported in the Sm-A phase of 8CB LC [29].
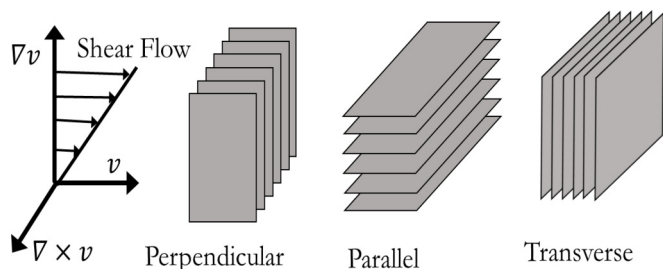
FIG. 3. Schematic representation of pseudolayer orientations in a shear flow.

The flow curve of N_{TB} phase has been studied and compared with that of the Sm-A phase of 8CB, as shown in Fig. 2(b). The N_{TB} phase shows a yield stress similar to that of the Sm-A phase of 8CB LC. However, the rheology of the Sm-A phase of 8CB is complex as it shows a shear-induced structural transition [30]. A small but discontinuous change in σ_{eff} near $\dot{\gamma} = 8$ s^{-1} in Fig. 2(b) and an increase in η_{eff} at 24 °C [Fig. 2(a)] could be a signature of such an effect. Interestingly, a similar discontinuity is observed in the case of CB9CB at $\dot{\gamma} = 22$ s^{-1}. Further studies are required to confirm the occurrence of such a transition in CB9CB. Nevertheless, the shear-rate-dependent shear stress σ_{eff} is fitted with the Herschel-Bulkley (HB) model:

$$\sigma_{eff} = \sigma_y + A\dot{\gamma}^n, \qquad (2)$$

where σ_y is the yield stress and A and n are constants. The fit parameters obtained are $n = 0.71$, $\sigma_y = 1.0$ Pa, $A = 1.9$ for N_{TB} and $n = 0.66$, $\sigma_y = 7.1$ Pa, $A = 2.9$ for the Sm-A phase. The two sets of fit parameters characterizing the flow curves of the two phases are reasonably close, suggesting they have similar flow behaviors. These two samples have structural similarity; namely, the pseudolayer thickness (∼10 nm) of the twist-bend nematic is close to the layer thickness of 8CB (∼2 nm). Moreover, both samples exhibit focal conic textures. Hence, their generic mechanical responses under shear are similar.

As a next step, we measure the dynamic modulus $G^*(\omega) = G'(\omega) + iG''(\omega)$. The regime of linear viscoelasticity of N_{TB} is determined by performing oscillatory measurements in which the strain amplitude varies from $\gamma = 0.01\%$ to $\gamma = 100\%$ at a fixed frequency $\omega = 1$ rad/s. The strain amplitude dependence can be described by the empirical relation [31]

$$G'(\omega, \gamma) = \frac{G'(\omega, 0)}{1 + \gamma/\gamma_c}, \qquad (3)$$

where γ_c is the critical strain amplitude. As shown in Fig. 4(a), the critical strain amplitude $\gamma_c = 3.3\%$, and the modulus $G'(1, 0) = 391$ Pa, setting the upper limit of the linear viscoelastic regime. For comparison we also measured G^* of the Sm-A phase of 8CB, shown in Fig. 4(a). It is interesting to note that not only the strain dependence but also the magnitudes of the shear moduli of N_{TB} and Sm-A are comparable, indicating they have common structural origin. Further, we have measured the temperature dependence of dynamic moduli of N_{TB} at a fixed shear amplitude $\gamma = 0.1\%$ and observed that $G' > G''$ in the entire N_{TB} phase [Fig. 4(b)], which is remarkably similar to that is observed in smectics with a true mass
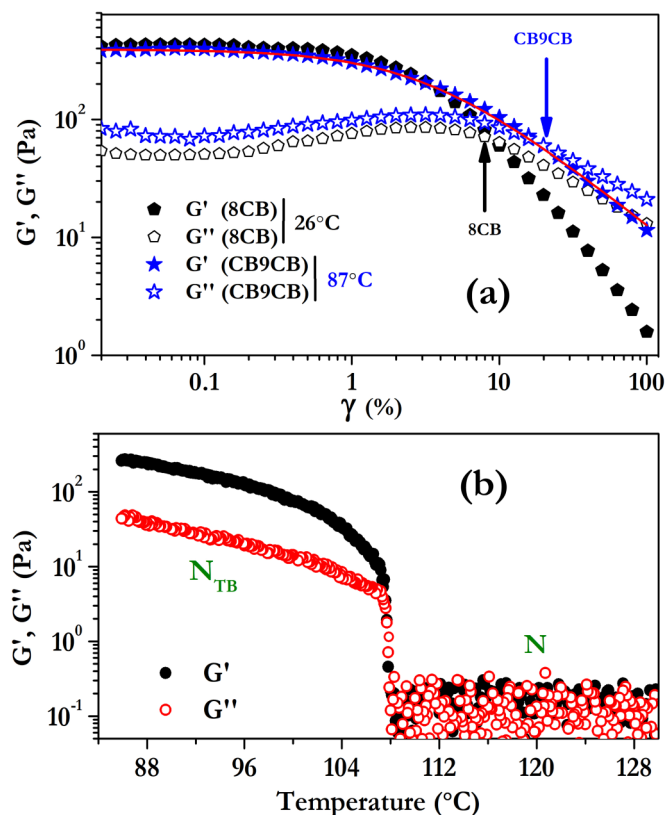

FIG. 4. (a) Strain amplitude dependence of the storage G' (solid symbols) and loss moduli G'' (open symbols) for N_{TB} ($T = 87$ °C) and 8CB ($T = 26$ °C). The solid line is a theoretical fit to Eq. (3). Arrows indicate crossover strains. (b) Temperature dependence of G' (solid symbols) and loss moduli G'' (open symbols) at a fixed strain amplitude $\gamma = 0.1\%$. Measurements are performed at frequency $\omega = 1$ rad/s.

density wave. Hence, the shear response of the N_{TB} phase can be discussed in analogy to the rheological responses of the usual Sm-A liquid crystals [31]. Like Sm-A, N_{TB} is solidlike in one direction and liquidlike in the other two directions. The three simplest orientations of the pseudolayers are considered, as shown in Fig. 3. In perpendicular and parallel orientations the pseudolayers can slide past each other easily, and the N_{TB} phase behaves like a liquid. In the transverse orientation the shear tends to change the pseudolayer spacing. As a result, the N_{TB} phase shows a viscoelastic solidlike behavior, and consequently, $G' > G''$.

The observed solidlike response of the N_{TB} phase can be explained based on a simple physical model described for defect-mediated cholesteric and smectic LCs. According to this model, the storage modulus can be expressed as [32]

$$G'(\omega) = G_0 + \beta_d \omega^{1/2} + \beta_0 \omega^2. \qquad (4)$$

The first term, G_0, arises from the elasticity of the static defects [33]. The second term, $\beta_d \omega^{1/2}$, arises from the regions of misaligned pseudolayers in the sample [34]. The last term results from the regions of the sample where the pseudolayers are parallel to the shear direction. The proportionality constants are given by $\beta_0 \simeq \eta(\gamma_1/K)(p/4\pi)^2$ and $\beta_d = (\pi/24\sqrt{2})\sqrt{(B_{eff}\eta)}$, where γ_1 is the rotational viscosity,
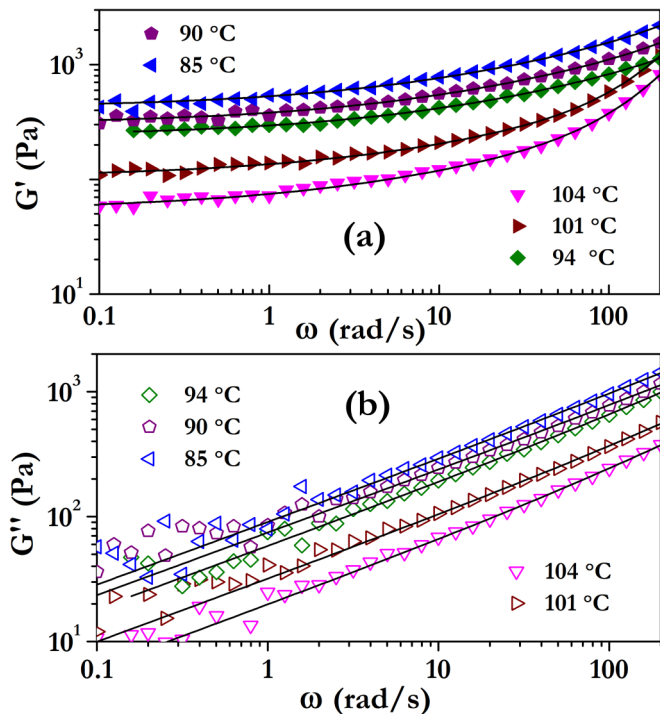
FIG. 5. Frequency dependence of storage G' (solid symbols) and loss G'' (open symbols) moduli at a few representative temperatures. Solid lines are theoretical fits of Eqs. (4) and (5) to G' and G'', respectively.
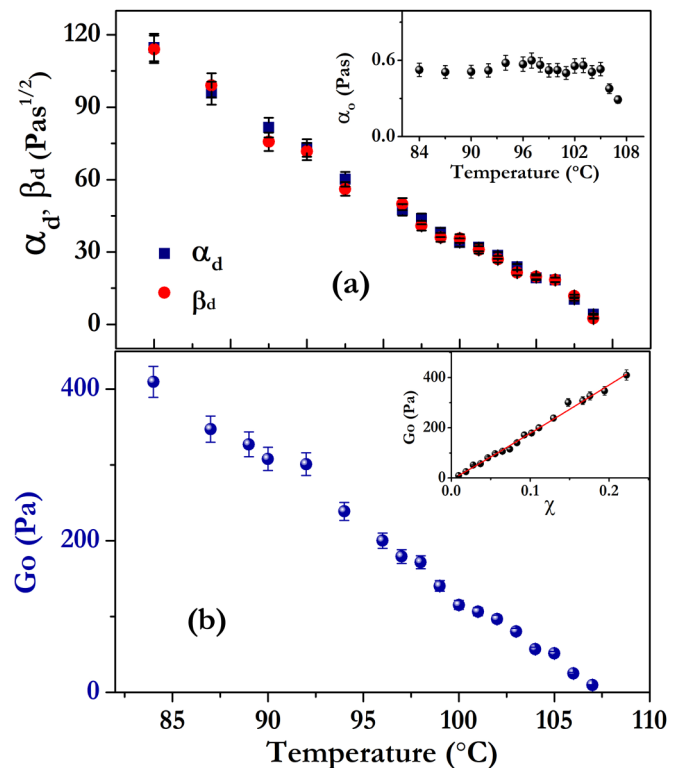

FIG. 6. (a) Temperature dependence of fit parameters β_d (red spheres) and α_d (navy blue squares). Inset: Temperature dependence of α_0. (b) Temperature dependence of the fit parameter G_0. Inset: The solid line shows the fit result $G_0 \sim \chi$, where the reduced temperature $\chi = (T_{TB} - T)/T_{TB}$.

η is the effective viscosity, and B_{eff} is the compression elastic modulus [34]. In particular, β_d describes the response of the lamellar regions with the layer normal oriented such that strain involves layer compression. Following similar arguments, the loss modulus can be written as [32]

$$G''(\omega) = \alpha_d \omega^{1/2} + \alpha_0 \omega, \tag{5}$$

where the first and second terms arise from the misaligned parts of the samples and the Maxwell-fluid-type contribution, respectively. Thus, by measuring β_d and α_0 from the disoriented sample, we can estimate B_{eff}. In order to measure these parameters at different temperatures we quenched the sample directly from the isotropic to the N_{TB} phase to obtain a mostly disoriented sample. Figure 5 shows some representative plots of $G'(\omega)$ and $G''(\omega)$ at different temperatures in the N_{TB} phase. The parameters obtained by fitting Eqs. (4) and (5) at different temperatures are shown in Fig. 6. The fit parameter β_0 is found to be very small (10^{-3}) and does not vary considerably with temperature. It is noted that $\beta_d \simeq \alpha_d$, as expected theoretically, and both increase with decreasing temperature. Assuming the whole sample is in the disorientated state, the temperature dependence of B_{eff} can be expressed as

$$B_{eff} = \frac{\beta_d^2}{\alpha_0} \left(\frac{24\sqrt{2}}{\pi} \right)^2. \tag{6}$$

Figure 7 shows the temperature dependence of calculated B_{eff} in the N_{TB} phase. Just below the N-N_{TB} transition B_{eff} is relatively smaller, 1.5×10^3 Pa $(T = 105\,°C)$, and it increases rapidly to 2×10^6 Pa $(T = 85\,°C)$. The latter value is only

one order of magnitude lower than the typical layer compression modulus of the Sm-A phase of 8CB [35]. So far, experimentally, B_{eff} of very few N_{TB} LCs have been measured. Gorecka *et al.* measured the temperature dependence of B_{eff} of a few chiral twist-bend nematic LCs, including CB7CB, using the atomic force microscopy technique and
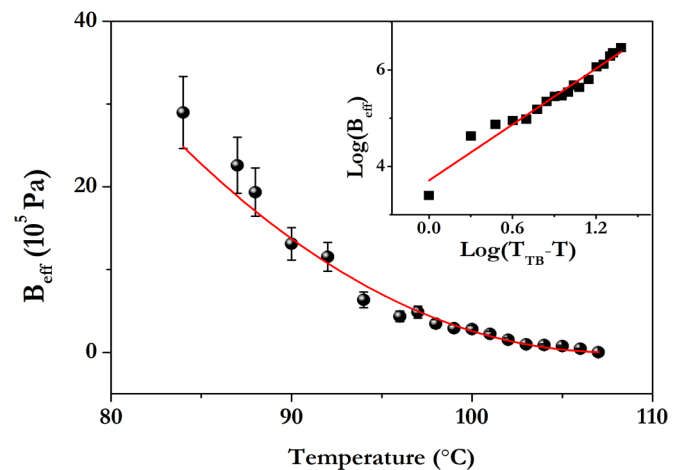

FIG. 7. Temperature dependence of effective elastic compressional modulus B_{eff}. The solid line is a theoretical fit to the equation $B_{eff} \sim (T_{TB} - T)^\alpha$, where $\alpha = 2.0 \pm 0.1$. Inset: Log-log scale.

reported that B_{eff} is in the range of 10^6–10^7 Pa, comparable to an ordinary Sm-A LC. Using a dynamic light-scattering technique, Parsouzi $et\ al.$ reported that B_{eff} of the N_{TB} phase of a LC made of a multicomponent mixture is in the range of 10^3–10^4 Pa, which is almost three orders of magnitude smaller than the ordinary Sm-A LCs [23,25]. Our experiment shows a wide variation of B_{eff}, covering both ranges. Such a wide variation of B_{eff} could partly be attributed to the increase in the cone angle θ with decreasing temperature. Based on a crude model, $B_{\text{eff}} = K_2(2\pi/p)^2\sin^4\theta$ [25], where θ increases with decreasing temperature [19,36]. Considering physical parameters for CB7CB such as $p = 10\,$nm [19] and $\theta = 10°$ [36] ($2\,°$C below the N-N_{TB} transition), $p = 8\,$nm [19] and $\theta = 33°$ [36] ($25\,°$C below the transition), and $K_2 = 3\,$pN, the calculated B_{eff} near two limiting temperatures are given by 1.1×10^3 and 1.6×10^5 Pa. The calculated B_{eff} close to the transition agrees reasonably well with our experiments, but it is smaller by one order of magnitude far below the transition. This assessment suggests that merely increasing the cone angle with decreasing temperature can enhance B_{eff} by almost two orders of magnitude.

The temperature dependence of B_{eff} was predicted theoretically using coarse-grained theoretical models. In analogy with Sm-A^*, Meyer and Dosov defined smecticlike effective pseudolayer compression and bending elastic constants K_{33}^N [22]. Assuming $K_{33}^N < 0$, they predicted $B_{\text{eff}} \sim (T_{\text{TB}} - T)^2$. Parsouzi $et\ al.$ developed another model accounting for the helical polarization field and its coupling with the bend distortion of the director [23]. Considering a small variation in the pseudolayer spacing and resulting changes in the cone angle and polar order, the theory predicts that there are two regimes of B_{eff}. For temperature T sufficiently close to T_{TB}, $B_{\text{eff}} \sim (T_{\text{TB}} - T)^3$, whereas for T sufficiently below T_{TB}, the theory gives $B_{\text{eff}} \sim (T_{\text{TB}} - T)^{3/2}$. Experimentally, they found (in a mixture exhibiting the N_{TB} phase) that within a relatively small temperature range ($\sim$6 °C), B_{eff} scales as $(T_{\text{TB}} - T)^{3/2}$.

To get an estimation of the scaling exponent of B_{eff}, we fit our data to the equation $B_{\text{eff}} \sim (T_{\text{TB}} - T)^\alpha$, with α being a fit parameter, as shown in Fig. 7. The inset shows the variation in the log-log scale. We obtain $\alpha = 2.0 \pm 0.1$, which is equal to the scaling exponent predicted by the "negative elasticity" model of Meyer and Dosov [22].

The temperature dependence of G_0 as shown in Fig. 6(b) indicates that the static defects contribute to a mechanical response of the N_{TB} phase similar to that of the Sm-A phase. The inset in Fig. 6(b) shows that G_0 scales with temperature as $G_0 \sim \chi$, where $\chi = (T_{\text{TB}} - T)/T_{\text{TB}}$ is the reduced temperature. This is slightly faster than that in the case of Sm-A ($\chi^{0.7}$)

[37], as expected in view of the fact that B scales much faster with temperature in the N_{TB} phase.

Three remarks are in order. First, in estimating β_d it has been assumed that the pseudolayers are disoriented in the whole sample. This assumption is reasonable as the sample was quenched from the isotropic phase to the twist-bend phase. Nevertheless, if the sample is partly oriented we do not expect an order of magnitude reduction of β_d and, consequently, B_{eff}. Following the same procedure, B_{eff} of 8CB is measured at a few temperatures, which agrees well with what was reported [35]. Second, the experimental results indicate that there are defects in our system whose contribution to the elasticity increases linearly with decreasing temperature. This might indicate a type-II N_{TB} having a twist grain boundary like structure as predicted by the coarse-grained model [22]. However, at this point we can say that more experimental investigations are required to draw any unambiguous conclusion. Last, it may be mentioned that although N_{TB} is structurally closer to cholesterics, the mechanical responses of N_{TB} and smectics are very much alike. This can be attributed to the fact that the thickness of pseudolayers in N_{TB} is much closer to the smectic layer than the pitch of the usual cholesterics.

IV. CONCLUSION

In this work we have presented rheological properties of a N_{TB} LC. The structural rheology of the N_{TB} phase is found to be remarkably similar to that of the usual Sm-A phase of calamitic liquid crystals. Our measurements revealed that in spite of the absence of a true mass density wave, N_{TB} LCs are viscoelastic solids similar to many defect-mediated lamellar systems. We found that B_{eff} is relatively softer near the N-N_{TB} transition but increases with decreasing temperature to three orders of magnitude more at a much faster rate than the usual Sm-A LCs. The temperature dependence of B_{eff} agrees well with the prediction of the coarse-grained elastic theories. Thus, our results provide a valuable test of the validity of the proposed theoretical models. This experiment also offer perspectives on N_{TB} LCs and open unexplored aspects of the rheology of nematic LCs with nanoscale modulation of the director.

[1] V. P. Panov, M. Nagaraj, J. K. Vij, Yu. P. Panarin, A. Kohlmeier, M. G. Tamba, R. A. Lewis, and G. H. Mehl, Phys. Rev. Lett. **105**, 167801 (2010).

[2] M. Čopič, Proc. Natl. Acad. Sci. U.S.A. **110**, 15855 (2013).

[3] D. Chen, J. H. Porada, J. B. Hooper, A. Klittnick, Y. Shena, M. R. Tuchbanda, E. Korblova, D. Bedrov, D. M. Walba, M. A. Glaser, J. E. Maclennana, and N. A. Clark, Proc. Natl. Acad. Sci. U.S.A. **110**, 15931 (2013).

[4] V. Borshch, Y.-K. Kim, J. Xiang, M. Gao, A. Jákli, V. P. Panov, J. K. Vij, C. T. Imrie, M. G. Tamba, G. H. Mehl, and O. D. Lavrentovich, Nat. Commun. **4**, 2635 (2013).

[5] L. Beguin, J. W. Emsley, M. Lelli, A. Lesage, G. R. Luckhurst,

B. A. Timimi, and H. Zimmermann, J. Chem. Phys. B **116**, 7940 (2012).

[6] G. Pajak, L. Longa, and A. Chrzanowska, Proc. Natl. Acad. Sci. U.S.A. **115**, E10303 (2018).

[7] J. Zhou, W. Tang, Y. Arakawa, H. Tsuji, and S. Aya, Phys. Chem. Chem. Phys. **22**, 9593 (2020).

[8] R. B. Meyer, in *Molecular Fluids*, edited by R. Balian and G. Weill, Les Houches Summer School in Theoretical Physics Vol. 25 (Gordon and Breach, New York, 1976), pp. 273–373.

[9] V. L. Lorman and B. Mettout, Phys. Rev. Lett. **82**, 940 (1999).

[10] V. L. Lorman and B. Mettout, Phys. Rev. E **69**, 061710 (2004).

[11] I. Dosov, Europhys. Lett. **56**, 247 (2001).

[12] R. J. Mandle, E. J. Davis, C. T. Archbold, S. J. Cowling, and J. W. Goodby, J. Mater Chem. C **2**, 556 (2014).

[13] M. Cestari, S. Diez-Berart, D. A. Dunmur, A. Ferrarini, M. R. de la Fuente, D. J. B. Jackson, D. O. Lopez, G. R. Luckhurst, M. A. Perez-Jubindo, R. M. Richardson, J. Salud, B. A. Timimi, and H. Zimmermann, Phys. Rev. E **84**, 031704 (2011).

[14] D. A. Paterson, J. P. Abberley, W. T. A. Harrison, J. M. D. Storey, and C. T. Imrie, Liq. Cryst. **44**, 127 (2017).

[15] C. Meyer, G. R. Luckhurst, and I. Dozov, Phys. Rev. Lett. **111**, 067801 (2013).

[16] N. Sebastian, B. Robles-Hernández, S. Diez-Berart, J. Salud, G. R. Luckhurst, D. A. Dunmur, D. O. López, and M. R. de la Fuente, Liq. Cryst. **44**, 177 (2017).

[17] N. Trbojevic, D. J. Read, and M. Nagaraj, Phys. Rev. E **96**, 052703 (2017).

[18] S. A. Pardaev, S. M. Shamid, M. G. Tamba, C. Welch, G. H. Mehl, J. T. Gleeson, D. W. Allender, J. V. Selinger, B. Ellman, A. Jakli, and S. Sprunt, Soft Matter **12**, 4472 (2016).

[19] C. Zhu, M. R. Tuchband, A. Young, A. Shuai, A. Scarbrough, D. M. Walba, J. E. Maclennan, C. Wang, A. Hexemer, and N. A. Clark, Phys. Rev. Lett. **116**, 147803 (2016).

[20] Z. Parsouzi, S. M. Shamid, V. Borshch, P. K. Challa, A. R. Baldwin, M. G. Tamba, C. Welch, G. H. Mehl, J. T. Gleeson, A. Jakli, O. D. Lavrentovich, D. W. Allender, J. V. Selinger, and S. Sprunt, Phys. Rev. X **6**, 021041 (2016).

[21] B. Robles-Hernández, N. Sebastián, M. R. de la Fuente, D. O. López, S. Diez-Berart, J. Salud, M. B. Ros, D. A. Dunmur, G. R. Luckhurst, and B. A. Timimi, Phys. Rev. E **92**, 062505 (2015).

[22] C. Meyer and I. Dosov, Soft Matter **12**, 574 (2016).

[23] Z. Parsouzi, S. A. Pardaev, C. Welch, Z. Ahmed, G. H. Mehl, A. R. Baldwin, J. T. Gleeson, O. D. Lavrentovich, D. W. Allender, J. V. Selinger, A. Jakli, and S. Sprunt, Phys. Chem. Chem. Phys. **18**, 31645 (2016).

[24] E. Gorecka, N. Vaupotic, A. Zep, D. Pociecha, J. Yoshioka, J. Yamamoto, and H. Takezoe, Angew. Chem., Int. Ed. **54**, 10155 (2015).

[25] S. M. Salili, C. Kim, S. Sprunt, J. T. Gleeson, O. Parri, and A. Jakli, RSC Adv. **4**, 57419 (2014).

[26] C. R. Safinya, E. B. Sirota, and R. J. Plano, Phys. Rev. Lett. **66**, 1986 (1991).

[27] J. Ananthaiah, M. Rajeswari, V. S. S. Sastry, and S. Dhara, Eur. Phys. J. E **34**, 74 (2018).

[28] M. Praveen Kumar, D. Venkata Sai, and S. Dhara, Phys. Rev. E **98**, 062701 (2018).

[29] R. G. Larson, *The Structure and Rheology of Complex Fluids* (Oxford University Press, New York, 1999), p. 480.

[30] P. Panizza, P. Archambault, and D. Roux, J. Phys. II **5**, 303 (1995).

[31] R. H. Colby, C. K. Ober, J. R. Gillmor, R. W. Connelly, T. Doung, G. Galli, and M. Laus, Rheol. Acta **36**, 498 (1997).

[32] L. Ramos, M. Zapotocky, T. C. Lubensky, and D. A. Weitz, Phys. Rev. E **66**, 031711 (2002).

[33] R. Bandyopadhyay, D. Liang, R. H. Colby, J. L. Harden, and R. L. Leheny, Phys. Rev. Lett. **94**, 107801 (2005).

[34] K. Kawasaki and A. Onuki, Phys. Rev. A **42**, 3664(R) (1990).

[35] M. Benzekri, J. P. Marcerou, H. T. Nguyen, and J. C. Rouillon, Phys. Rev. B **41**, 9032 (1990).

[36] C. Meyer, G. R. Luckhurst, and I. Dosov, J. Mater. Chem. C **3**, 318 (2015).

[37] S. Fujii, S. Komura, Y. Ishii, and C.-Y. D. Lu, J. Phys.: Condens. Matter **23**, 235105 (2011).